Synthesis of $CuInGaSe_2$ Nanoparticles by Low Temperature Colloidal Route

Ki-Hyun Kim, Young-Gab Chun, Kyung-Hoon Yoon*
Solar Cells Research Center, Korea Institute of Energy Research, 71-2 Jang-dong, Yusong-gu, Daejon 305-343, Korea
Byung-Ok Park
Department of Inorganic Materials Engineering, Kyungpook National University, 1370 Sankyuk-dong, Puk-ku, Daegu 702-701, Korea

CIGS nanoparticles were synthesized by a low temperature colloidal route for the absorber layer of photovoltaic devices. The CIGS nanoparticles were prepared by reacting CuI, InI_3, GaI_3 in pyridine with Na_2Se in methanol at 0℃ under inert atmosphere. The reaction products of dark red and yellow colors were turned out to be NaI and CIGS nanoparticles, respectively, by ICP-AES and SEM-EDS analyses. Chalcopyrite structure of the CIGS nanoparticles was confirmed by XRD and TEM diffraction patterns. As compared to the particles from $Cu_{0.9}In_{0.8}Ga_{0.3}Se_2$ ratio, more uniform and smaller nanoparticles were obtained from $Cu_{1.1}In_{0.68}Ga_{0.23}Se_{1.91}$ stoichiometric ratio. The CIGS nanoparticles were measured to be in the ranges of 5-20 nm. However, tube like CIGS particles with length of several μm and width in the range of 100-300 nm were obtained from $Cu_{0.9}In_{0.8}Ga_{0.3}Se_2$, and $Cu_{0.9}In_{0.7}Ga_{0.4}Se_2$. The morphological change of the CIGS particles seems to be closely related to the ratio of Cu/(In+Ga).

Key Words : Solar cell, $CuInGaSe_2$, Absorber layer, Nanoparticles

1. Introduction

Conversion of solar energy into electricity and heat using photovoltaic or solar thermal methods were studied by several groups (Hong, 2005 ; Seo et al., 2003) The solar cell is very important in the photovoltaic system. Compound solar cell devices consist of electrode/transparent conducting oxides (TCO)/buffer layer/absorber layer/back contact/soda-lime glass. Figure 1 shows the structure of CIGS compound semiconductor solar cells. In general, chalcopyrite material of $CuInGaSe_2$ (CIGS) is known to be a very prominent absorber layer for high efficiency and low cost thin film solar cell devices. A solar energy to electrical energy conversion efficiency over 19%

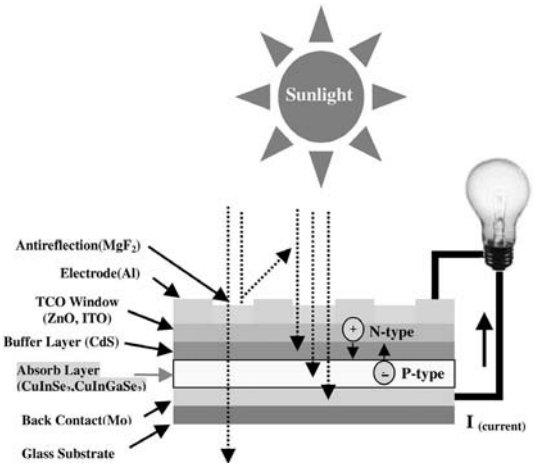

Fig. 1 The structure of CIGS compound semiconductor solar cells

* Corresponding Author,
E-mail : y-kh@kier.re.kr
TEL : +82-42-860-3191; **FAX** : +82-42-860-3739
Solar Cells Research Center, Korea Institute of Energy Research, 71-2 Jang-dong, Yusong-gu, Daejon 305-343, Korea. (Manuscript **Received** January 25, 2005; **Revised** May 13, 2005)

has recently been reported for a small area (0.41 cm^2) CIGS devices (Rockett and Birkmire, 1991 ; Ramanathan et al., 2003). While this CIGS device possesses the highest thin film polycrystalline solar cell efficiency to date, the scaling of this technology toward commercialization presents many challenges. Most of the research groups developing CIGS solar cells have used physical vapor deposition (PVD) techniques such as evaporation (Rockett and Birkmire, 1991) or sputtering (Parretta et al., 1998) for depositing the absorber layer of CIGS. However, it is expensive to manufacture photovoltaic (PV) device by PVD method and it is difficult with almost of these methods to obtain satisfactory stoichiometric compound. To solve such problem, various processes are being tried for making CIGS absorber layer. Spray deposition process has been employed using CIGS nanoparticles in low temperature processes for solar cells. In this work, we have tried a novel approach to fabricate CIGS solar cells in which a non-vacuum process is used for depositing the CIGS absorber layer. We synthesized CIGS nanoparticles for the CIGS absorber layer of solar cells by colloidal route. We address some characteristic features and the morphology change of the obtained CIGS particles according to the ratio of Cu/(In+Ga).

2. Experimental

We have recently reported the synthesis of CIGS nanoparticles for the CIGS absorber layer by solvothermal routes (Kim et al., 2004) We obtained the spherical CIGS nanoaprticles at reaction temperatures over 230℃ by solvothermal routes. In the case of colloidal method, it was reported that the synthesis of the CIGS particles was carried out at a low temperature such as 0℃ (Schulz et al., 1998a ; 1998b). The experimental procedure for CIGS nanoparticles synthesis by colloidal route is briefly sketched in Fig. 2.

The CIGS nanoparticles were prepared by reacting CuI, InI_3, GaI_3 in pyridine with Na_2Se in methanol at 0℃ in a glove box under inert atmosphere. The pyridine and methanol were distilled and deoxygenated before use. The metal

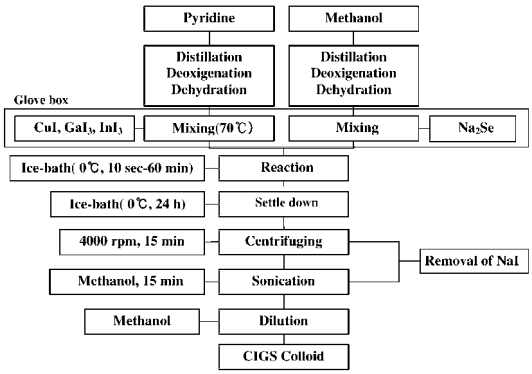

Fig. 2 Experimental procedure for CIGS nanoparticles synthesis by colloidal route

iodines of CuI, InI_3, and GaI_3 and Na_2Se were dissolved in the pyridine and methanol solvents, respectively. The pyridine solution was mixed with the methanol solution. The solution mixture was reacted with stirring for the reaction times in the range from 10 seconds to 1 hour in ice bath at 0℃. The reaction mixture was allowed to settle down for 24 hours and then, the reaction product of dark red color supernatant was decanted and discarded. Thereafter, the remaining reaction products were transferred to 50 ml centrifuge tube, which was added with distilled and deoxygenated methanol to fill it. Then, it was subjected to sonication for 10 minutes. The products of yellow color were centrifuged for 10 minutes at 4000 rpm. At the completion of centrifugation, the reaction products of dark red and yellow colors were turned out to be NaI and CIGS nanoparticles, respectively, by inductively coupled plasma atomic emission spectrometer (ICP-AES : Ultima-C, Jobin Yyon, France) and energy dispersive spectrometry (EDS : Phoenix, EDAX Inc., USA) analyses. The particle size and the morphology of the products were investigated by high-resolution scanning electron microscopy (HRSEM : XL30SFEG, Philips Co., Holland at 10 kV) and transmission electron microscopy (TEM : EM912Ω, Carl Zeiss Co., Germany). The phase and the crystallographic structure of the products were identified by X-ray diffraction (XRD : D/max-A, Rigaku, Japan, Cu Kα : λ=1.54178 Å) and TEM.

3. Results and Discussions

In order to obtain spherical CIGS particles, the colloidal route reactions were carried out in ice-bath as a function of reaction times and Cu/(In+Ga) ratios of raw material. First of all, in order to obtain the information about the chemical composition of the nanoparticles, every product was analyzed with EDS (Fig. 3).

The average atomic composition of the surface of the nanoparticles was determined to be approximately a ratio of 1.1 : 0.9 : 1.91 for Cu : In+Ga : Se. The chemical composition of the reaction product of dark red color supernatant obtained from the reactions in ice-bath for 20 minutes was determined with ICP-AES and given in Table 1.

Figure 4 shows photo images illustrating the reaction at low temperature and the reaction products after settle-down. Three parts of the slurry were separated to the top, middle and bottom layers. The colors of the separated slurry layers were orange, yellow and gray. The middle layer of yellow color became the highest quantity compared to the other slurry layers from settle-down for 24 hours.

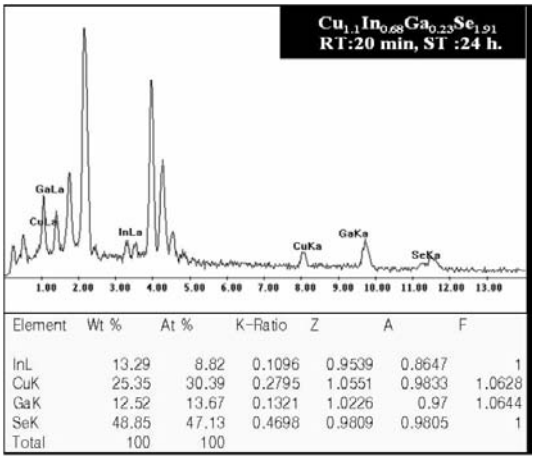

Element	Wt %	At %	K-Ratio	Z	A	F
InL	13.29	8.82	0.1096	0.9539	0.8647	1
CuK	25.35	30.39	0.2795	1.0551	0.9833	1.0628
GaK	12.52	13.67	0.1321	1.0226	0.97	1.0644
SeK	48.85	47.13	0.4698	0.9809	0.9805	1
Total	100	100				

Fig. 3 EDS image of the middle layer products obtained from the reaction in ice-bath for 20 minutes

Table 1 Chemical compositions of the reaction product of dark red color supernatant

Element	Na	I	Cu
Atom%	30.14	55.83	14.83

Figure 5 shows the reaction products of spherical morphologies obtained from settle-down for 24 hours. The middle layer of yellow color has very fine and uniform nanoparticles with diameter below 15 nm as shown in Fig. 5(b).

Figure 6 shows XRD diffraction patterns of the slurry. For $Cu_{1.1}In_{0.68}Ga_{0.23}Se_{1.91}$ stoichiometric ratio, the top slurry layer showed only weak (112) peak. On the other hand, the middle and bottom slurry layers slurry showed typical XRD patterns for the chalcopyrite structure of the

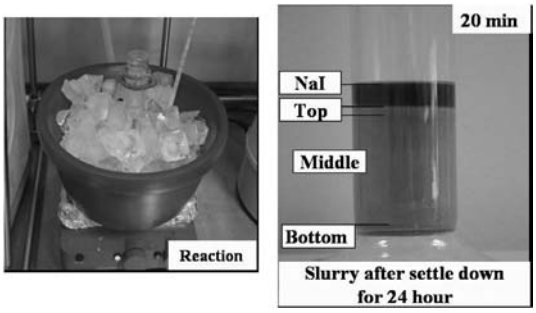

Fig. 4 Photo images of the reaction flask subjected to ice-bath at 0℃ for 20 minutes and the slurry product separated from settle-down for 24 hours

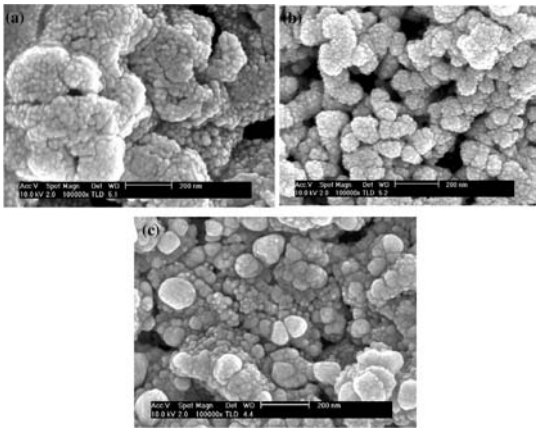

Fig. 5 SEM images of CIGS colloidal separated from settle-down for 24 hours: (a) top, (b) middle and (c) bottom layer

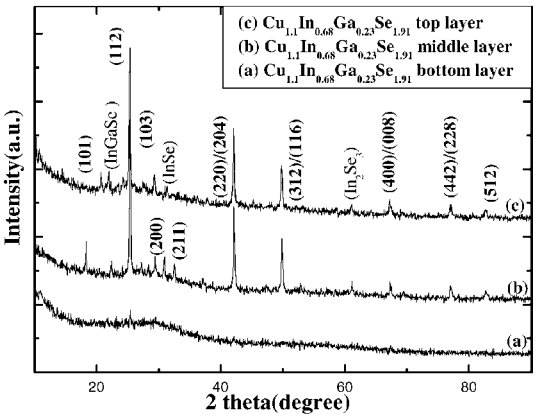

Fig. 6 XRD diffraction patterns of the slurry layers separated from the reaction product of $Cu_{1.1}In_{0.68}Ga_{0.23}Se_{1.91}$

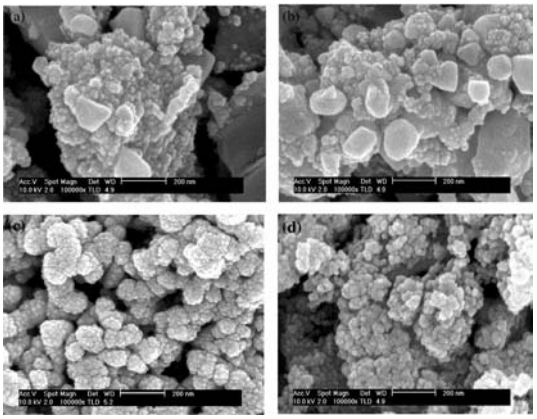

Fig. 7 SEM images of the $Cu_{1.1}In_{0.68}Ga_{0.23}Se_{1.91}$ nanoparticles obtained from the reaction with stirring in ice bath for various reaction times: (a) 10 sec, (b) 1 minute, (c) 20 minutes and (d) 60 minutes

reaction products obtained from the separated CIGS (Fig. 6). Both layers exhibited an intense peak at $2\theta=26.6°$ oriented along the (112) direction. The other prominent peaks corresponded to the (220)/(204) and (312)/(116) directions. In addition to these commonly observed orientations, the weak peaks such as (400)/(008), (442)/(228) and (512) were also observed in the XRD patterns. In addition, the various peaks related to the presence of $InGaSe_2$, In_2Se_3 and InSe phase were observed.

Figure 7 shows SEM images of the $Cu_{1.1}In_{0.68}Ga_{0.23}Se_{1.91}$ nanoparticles obtained from the reaction in ice bath at 0℃ for various reaction times. The reaction time of 20 minutes led to the most spherical nanoparticles in which, fine and uniform nanoparticles with diameter below 20 nm agglomerate into larger particles. For the reaction times of 10 seconds and 1 minute, plate-type and spherical particles were mixed with diameter below sub-micron meter as shown in Fig. 7(a) and (b). For the reaction time of 60 minutes, the $Cu_{1.1}In_{0.68}Ga_{0.23}Se_{1.91}$ particles were observed to be bigger and irregular than those for 20 minutes.

Figure 8 shows typical XRD patterns for the CIGS nanoparticles of $Cu_{1.1}In_{0.68}Ga_{0.23}Se_{1.91}$ stoichiometric ratio obtained from the reactions for various reaction times. For the reaction times of 10 sec and 1 minute, the XRD patterns of the

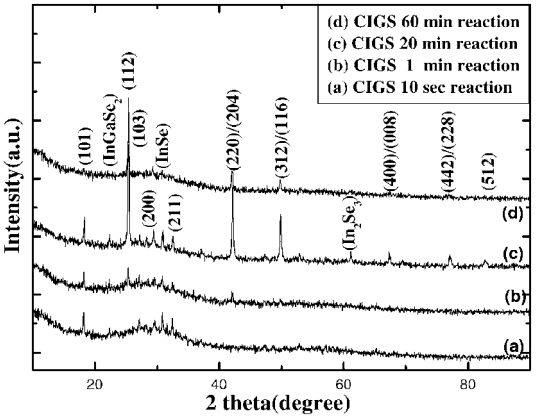

Fig. 8 XRD patterns of the CIGS nanoparticles obtained from the reaction in ice-bath for various reaction times: (a) 10 sec, (b) 1, (c) 20 and (d) 60 minutes

CIGS phase is relatively weak. This is indicative that the formation reaction did not proceed completely for the reaction times. For the reaction times over 20 minutes, typical patterns of the CIGS were obtained. Therefore, we used the reaction time of 20 minutes as optimum reaction time for preparation of CIGS nanoparticles.

Figure 9 shows TEM image of small agglomerates of $Cu_{1.1}In_{0.68}Ga_{0.23}Se_{1.91}$ nanoparticles obtained from the reaction in ice-bath for 20 minutes. This confirmed that the spherical

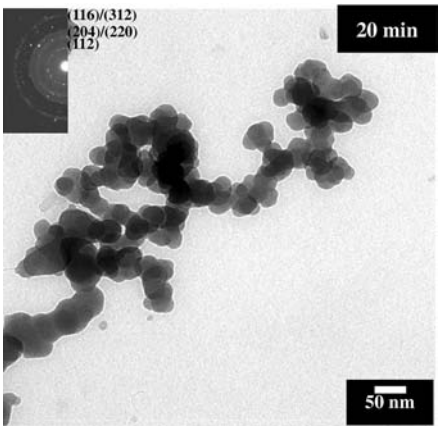

Fig. 9 TEM image of small agglomerates of $Cu_{1.1}In_{0.68}Ga_{0.23}Se_{1.91}$ nanoparticles obtained from the reaction in ice-bath for 20 minutes

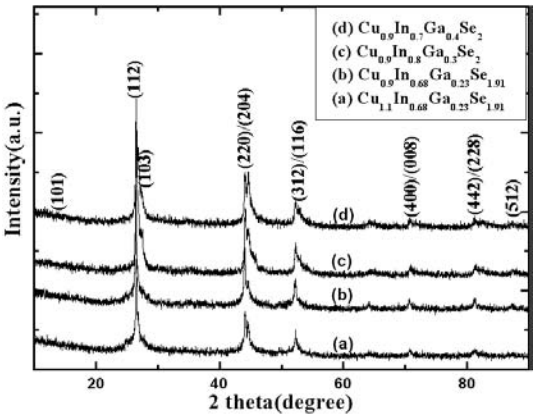

Fig. 11 XRD patterns for the CIGS particles of the various stoichiometric ratios: (a) $Cu_{1.1}In_{0.68}Ga_{0.32}Se_{1.91}$, (b) $Cu_{0.9}In_{0.68}Ga_{0.32}Se_{1.91}$, (c) $Cu_{0.9}In_{0.8}Ga_{0.3}Se_2$ and (d) $Cu_{0.9}In_{0.7}Ga_{0.4}Se_2$

$Cu_{1.1}In_{0.68}Ga_{0.23}Se_{1.91}$ nanoparticles of the small agglomerate with diameter in the range of 5-20 nm were obtained from the reaction in ice-bath reaction for 20 minutes. The electron diffraction patterns corresponded to the prominent peaks, (112), (204)/(220), (116)/(312) of the tetragonal CIGS phase.

Figure 10 shows SEM images of the CIGS particles obtained from the various stoichiometric ratios. As compared to the particles from $Cu_{0.9}In_{0.8}Ga_{0.3}Se_2$ ratio (Fig. 10(b)), more uniform and smaller nanoparticles were obtained from the $Cu_{1.1}In_{0.68}Ga_{0.23}Se_{1.91}$ stoichiometric ratio (Fig. 10(d)). The spherical CIGS nanoparticles were obtained from low ratios of Cu/(InGa), such as $Cu_{1.1}In_{0.68}Ga_{0.23}Se_{1.91}$, and $Cu_{0.9}In_{0.68}Ga_{0.23}Se_{1.91}$, whereas tube-like CIGS particles with length of several μm and width in the range of 100-200 nm were obtained from $Cu_{0.9}In_{0.8}Ga_{0.3}Se_2$ and $Cu_{0.9}In_{0.7}Ga_{0.4}Se_2$.

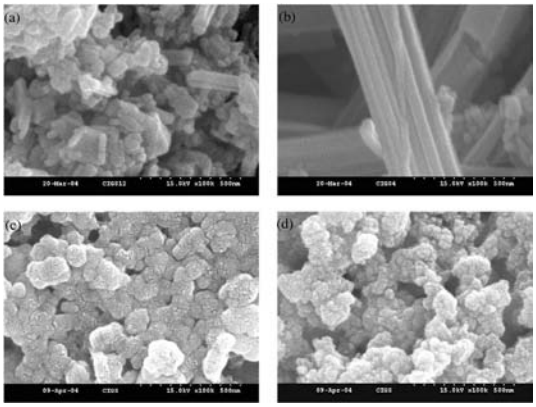

Fig. 10 SEM images for the CIGS particles of various stoichiometric ratios: (a) $Cu_{0.9}In_{0.7}Ga_{0.4}Se_2$, (b) $Cu_{0.9}In_{0.8}Ga_{0.3}Se_2$, (c) $Cu_{0.9}In_{0.68}Ga_{0.32}Se_{1.91}$ and (d) $Cu_{1.1}In_{0.68}Ga_{0.32}Se_{1.91}$

The examination of XRD was carried out on the tube-like particles to confirm CIGS tetragonal phase. Figure 11 shows XRD diffraction patterns for the CIGS particles of the various stoichiometric ratios. All the CIGS nanoparticles of various stoichiometric ratios showed a typical X-ray diffraction pattern for chalcopyrite structure with an intense peak at $2\theta=26.6°$ oriented along the (112) direction. The other prominent peaks corresponded to the (220)/(204) and (312)/(116) directions. In addition to these commonly observed orientations, the weak peaks such as (400)/(008), (442)/(228) and (512) were also observed in the XRD patterns. The presence of the peaks related to (400)/(008) direction implies that Ga takes partly the place of In in the tetragonal CIS phase and then results in the tetragonal CIGS phase.

4. Conclusion

The chalcopyrite CIGS nanoparticles with diameters in the range of 5-20 nm were prepared

by reacting CuI, InI_3, GaI_3 in pyridine with Na_2Se in methanol at 0℃ under the inert atmosphere within glove box by colloidal process. The morphological change of the CIGS particles depended on the ratio of Cu/(In+Ga). As the amount of the III family, i.e., (In+Ga) increased, the shape of CIGS nanoparticles changed from tube-like to spherical types. For $Cu_{0.9}In_{0.7}Ga_{0.4}Se_2$ stoichiometric ratio, tube-type particles were obtained from reaction at 0℃ for 20 min, and measured to be with the widths in the range of 100-300 nm and lengths of 1-5 μm. For $Cu_{1.1}In_{0.68}Ga_{0.23}Se_{1.91}$ and $Cu_{0.9}In_{0.8}Ga_{0.3}Se_2$ ratios, spherical nanoparticles were obtained at the same reaction condition as that of $Cu_{0.9}In_{0.7}Ga_{0.4}Se_2$ tube-type particles. As compared to the particles of $Cu_{1.1}In_{0.68}Ga_{0.23}Se_{1.911}$ ratio, more uniform and smaller nanoparticles with diameter in the range of 5-20 nm were obtained from the $Cu_{0.9}In_{0.68}Ga_{0.32}Se_{1.9}$ stoichiometric ratio.

Acknowledgments

The present work was supported by Korea Ministry of Science and Technology through National R&D Project for Nano Science and Technology.

References

Douglas, L. Schulz, Calvin, J. curtis, Rebecca, A. Flittion, Holm wiesner, James Keanw, Richard, J. Maston, Kim, M. Jones, Philp A. Parilia, Rommel Noufi, and David, S. Ginley, 1998a, *Journal of Electronic Materials*, Vol. 27, No. 5, pp. 433～437.

Douglas, L. Schulz, Calvin, J. Curtis, David, S. Ginley, 27, jan., 1998b, US. partent, patent No. 6, 126,740.

H. K. Hong, 2005, *Journal of the KSME*, Vol. 45, pp. 23～25

K.-H. Kim, Y.-G. Chun, B.-O. Park and K.-H., Yoon, 2004, *Mat. Sci. Forum*, 449-452, pp. 273～276.

A. Parretta, M. L. Addonizio, S. Loreti, L. Quercia and M. K. Jauaraj, 1998, *Journal of Crystal Growth* 183, pp. 196～204.

K. Ramanathan, M. A. Contreras, C. L. Perkins, S. Asher, F. S. Hasoon, J. Keane, D. Young, M. Romero, W. Metzger, R. Noufi, J. Ward and A. Duda, 2003, Prog. Photovolt: Res. Appl. 11, p. 225.

A. Rockett and R. W. Birkmire, 1991, *J. Appl. Phys*. 70, R81.

T. B. Seo, S. Y. Ryu and Y. H. Kang, 2003, *KSME International Journal*, Vol. 17, No. 8, pp. 1185～1195.